

Table S1. Summary of the number of samples (*N*) for all analyses, with technique or instrument used in parentheses.

Analysis	<i>N</i>							
Particle size analysis	12							
Mineralogy (XRD)	12							
Loss-on-ignition	12							
	HW	HW	HW	HW	MS	MS	MS	MS
	0-10 cm	30-40 cm	70-80 cm	110-120 cm	0-10 cm	30-40 cm	70-80 cm	110-120 cm
pH, DO, EC, T (YSI)	16	14	12	16	9	15	16	11
Al _{aq} (ICP-OES)	16	13	11	11	6	15	15	10
Fe _{aq} (ICP-OES)	4	14	12	16	8	15	16	10
Mn _{aq} (ICP-OES)	16	14	11	16	8	15	16	10
Cu _{aq} (ICP-OES)	16	14	3	5	4	7	4	5
Zn _{aq} (ICP-OES)	16	14	11	16	8	15	16	10
Ni _{aq} (ICP-OES)	16	12	11	16	8	15	16	10
DOC (TOC)	15	13	11	13	7	15	14	10
Cl _{aq} (IC)	13	11	7	15	7	13	13	10
SO ₄ ²⁻ _{aq} (IC)	12	10	7	12	7	12	11	9

Table S2. Particle size distribution (percent) and bulk mineralogical composition (weight percent) of the soil samples.

Particle Size Distribution							Mineral Abundance									
High Wall				Mine Spoil			High Wall					Mine Spoil				
Depth (cm)	clay	silt	sand	clay	silt	sand	quartz	feldspar ^a	kaolinite	muscovite	chlorite	quartz	feldspar ^a	kaolinite	muscovite	chlorite
0-10	4.7	54.1	41.2	7.2	47.8	45.0	41	6.8	13.6	36.6	2.1	34	3.7	20.5	38.6	3.2
10-20	4.6	51.9	43.5	7.1	44.4	48.4	34.5	6.1	14.9	41.4	3.3	27.5	3.5	21.7	45	2.3
20-30	3.2	37.6	59.2	5.4	45.0	49.6	35.1	8.3	14.2	39.3	3	41.9	4.2	16.5	35.3	2.1
30-40	3.6	41.4	55.0	5.4	43.3	51.3	43.3	6.5	12.3	34.9	3	49	3.8	16.1	29.1	2.1
40-50	4.6	48.6	46.8	5.4	42.3	52.3	37.8	6.5	13.1	38.8	3.8	41.7	6.5	18.6	30.9	2.4
50-60	4.6	51.2	44.2	5.1	38.0	56.9	30.6	8.7	15.3	42.6	2.9	34.3	6.2	20	35.4	3.9
60-70	4.7	47.9	47.4	5.6	35.7	58.7	38	6.9	14.6	37	3.5	34.6	6	18.8	36.5	5
70-80	4.8	48.6	46.5	6.2	39.7	54.0	35.6	3.9	15.5	42.3	2.6	44	4	17.9	33.3	0.8
80-90	4.1	43.2	52.7	7.2	44.5	48.3	38.9	5.7	13	38.4	3.9	34.7	1.1	22.4	38.1	3.7
90-100	4.5	47.0	48.5	6.5	42.2	51.2	37.5	6	15.3	38.5	2.6	37.3	4.8	19.9	33.4	4.6
100-110	4.4	48.8	46.8	7.4	40.4	52.3	36.3	5.4	15	39.3	4	28.7	4.5	20.8	38.1	7.8
110-120	4.8	52.6	42.6	6.7	38.5	54.7	34.8	5.9	14.3	41.6	3.4	31.1	9.4	18.3	40	1.1

a. The sum of albite + anorthite + orthoclase

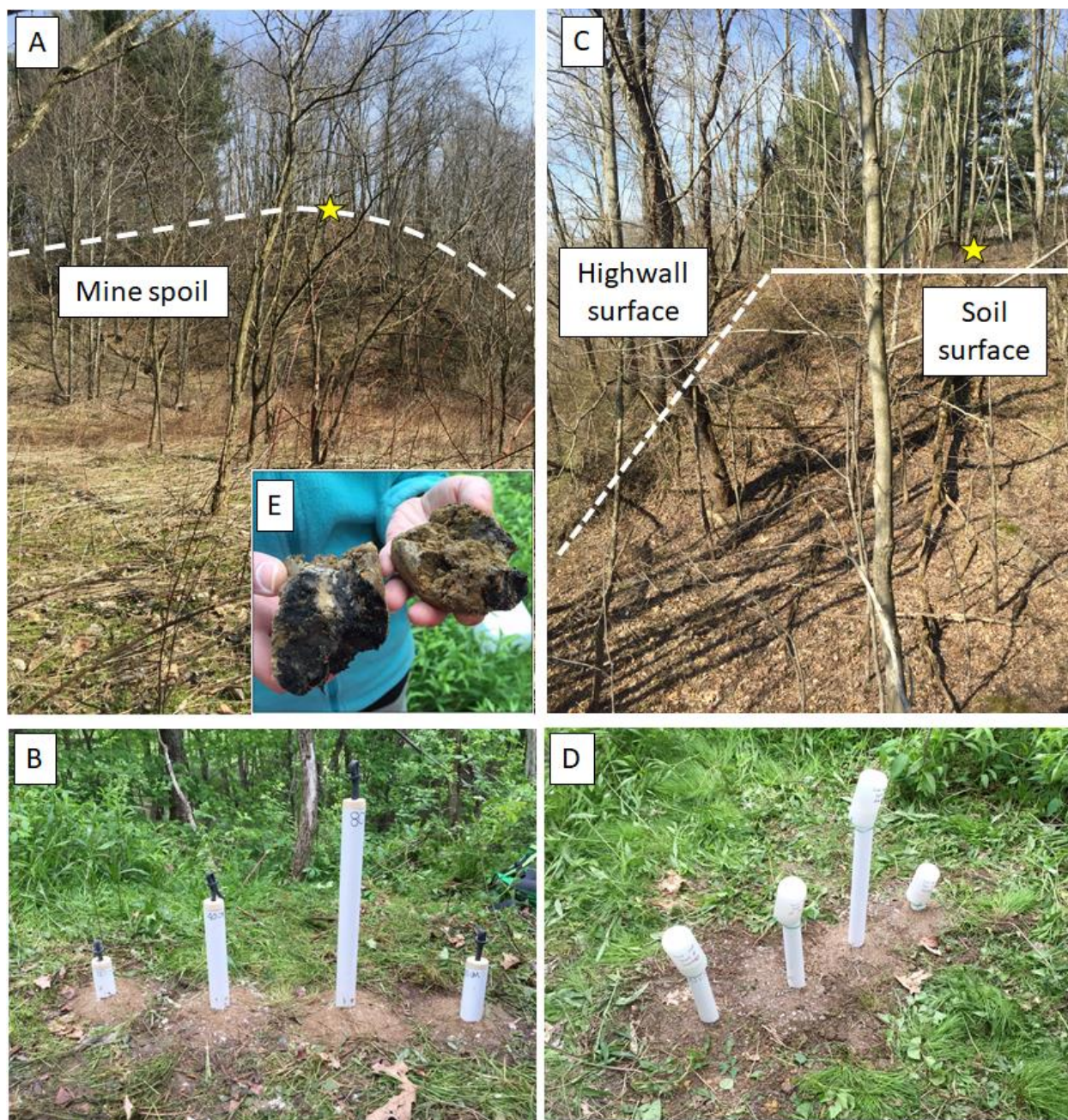


Figure S1. Photographs of the two soil sampling locations and post-installation lysimeters for the mine spoil (A and B) and high wall (C and D). The insert photograph (E) shows a characteristic mine spoil aggregate recovered during soil coring.

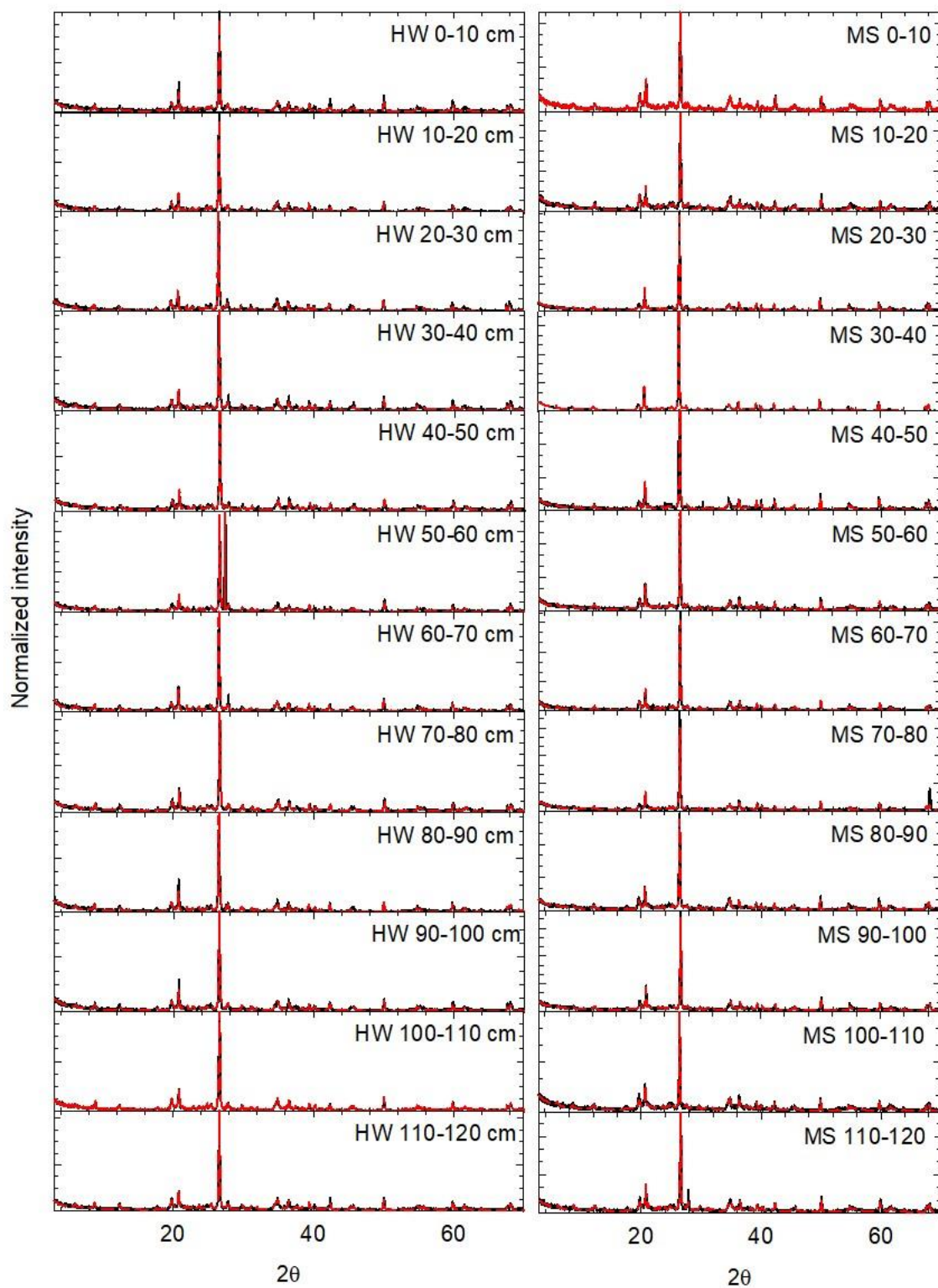


Figure S2. Background subtracted, normalized bulk XRD patterns (black solid lines) and fits (red dashed lines).

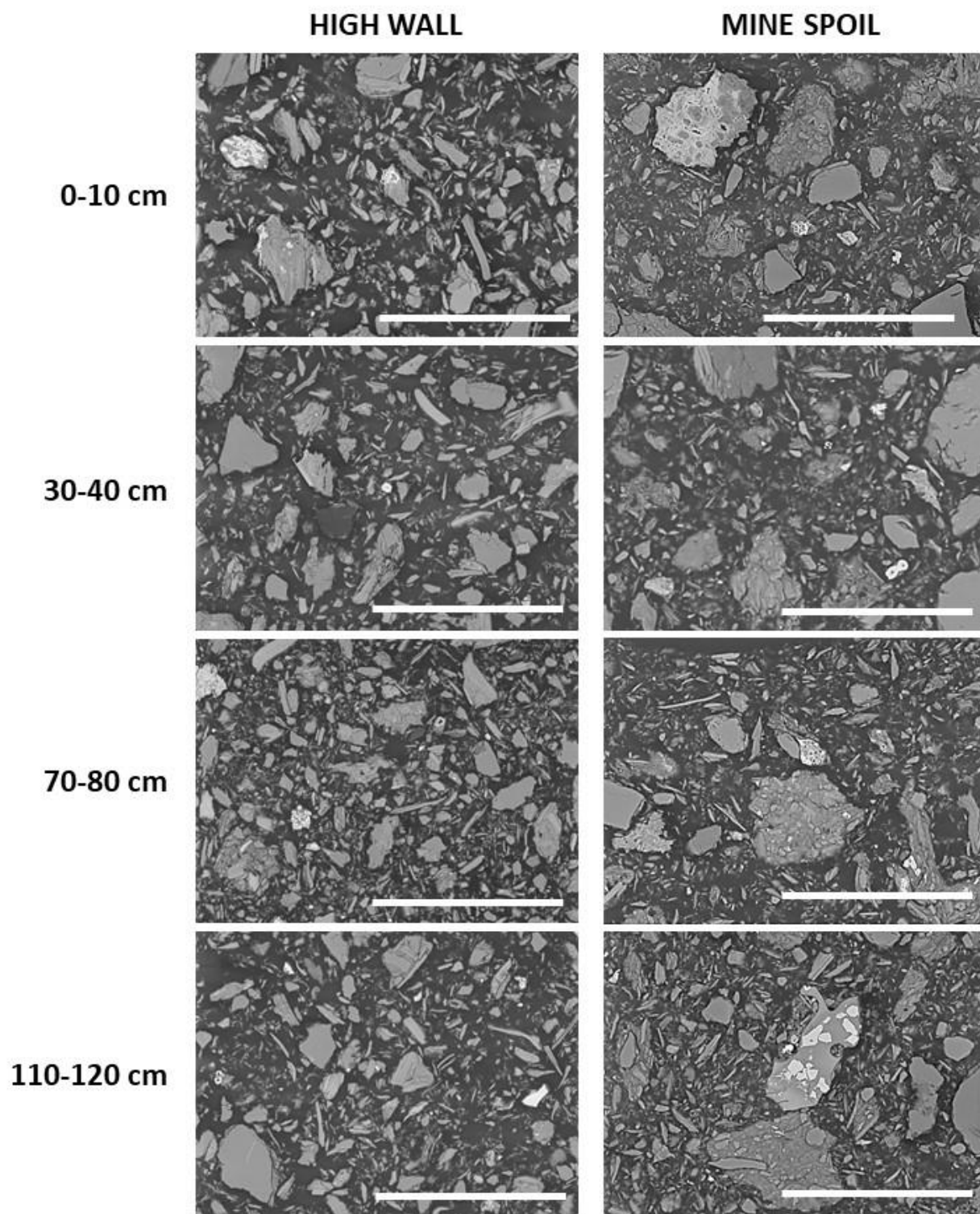


Figure S3. SEM images of High Wall (left) and Mine Spoil (right) soils from the four sampling depths. The scale bar for all images is 100 μm .

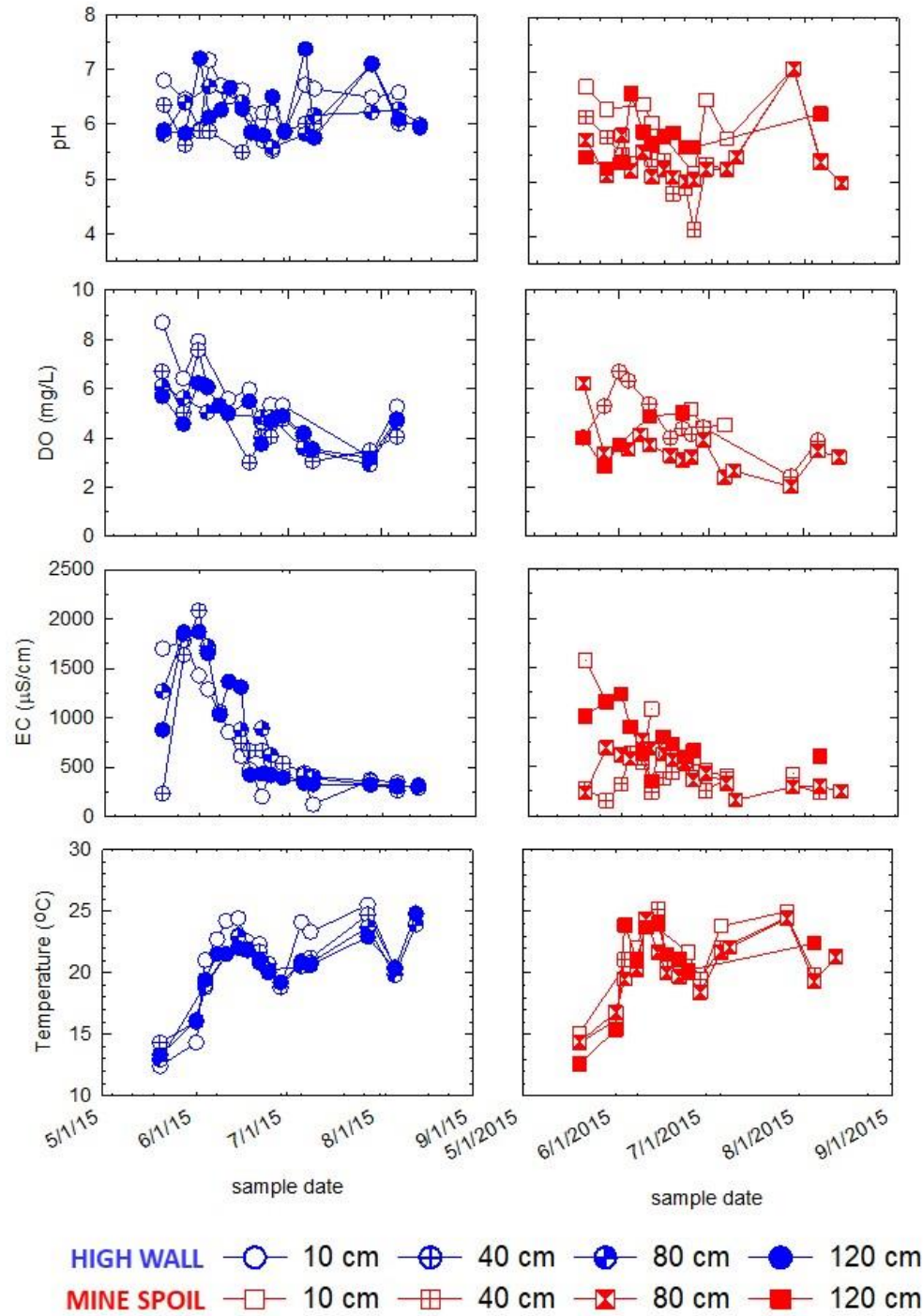


Figure S4. Field measurements of pH, dissolved oxygen (DO), electrical conductivity (EC), and temperature collected from lysimeters installed in High Wall soils (blue circles, left) and Mine Spoil soils (red squares, center) over the sampling season for lysimeters installed at 10 cm (open), 40 cm (cross), 80 cm (hour glass), and 120 cm (filled).

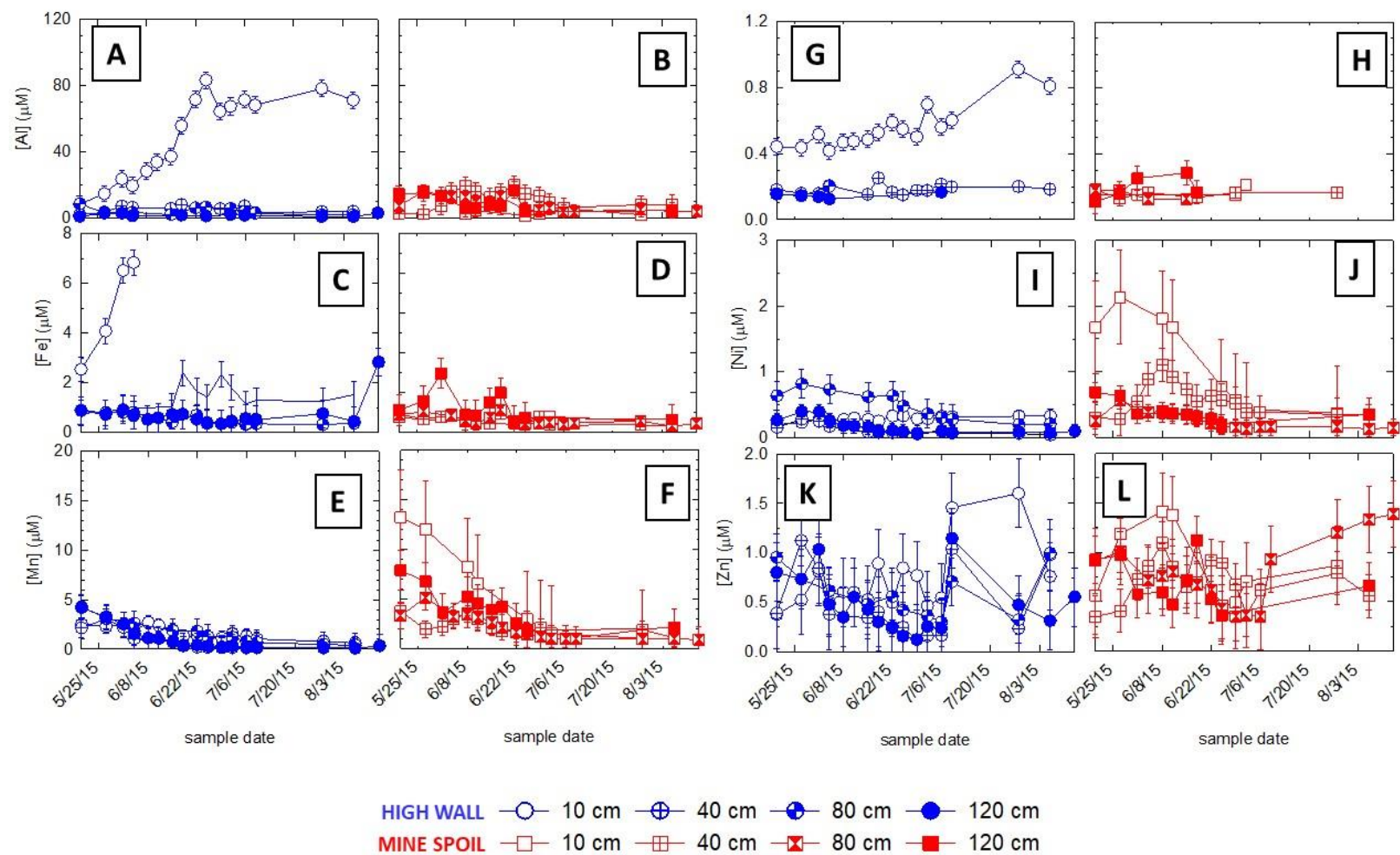


Figure S5. Aqueous concentrations of Al (A and B), Fe (C and D), Mn (E and F), Cu (G and H), Ni (I and J), and Zn (K and L) collected from lysimeters installed in high wall soils (blue symbols) and mine spoil soils (red symbols) over the sampling season for lysimeters installed at 10 cm (open), 40 cm (cross), 80 cm (hour glass), and 120 cm (filled) depth.

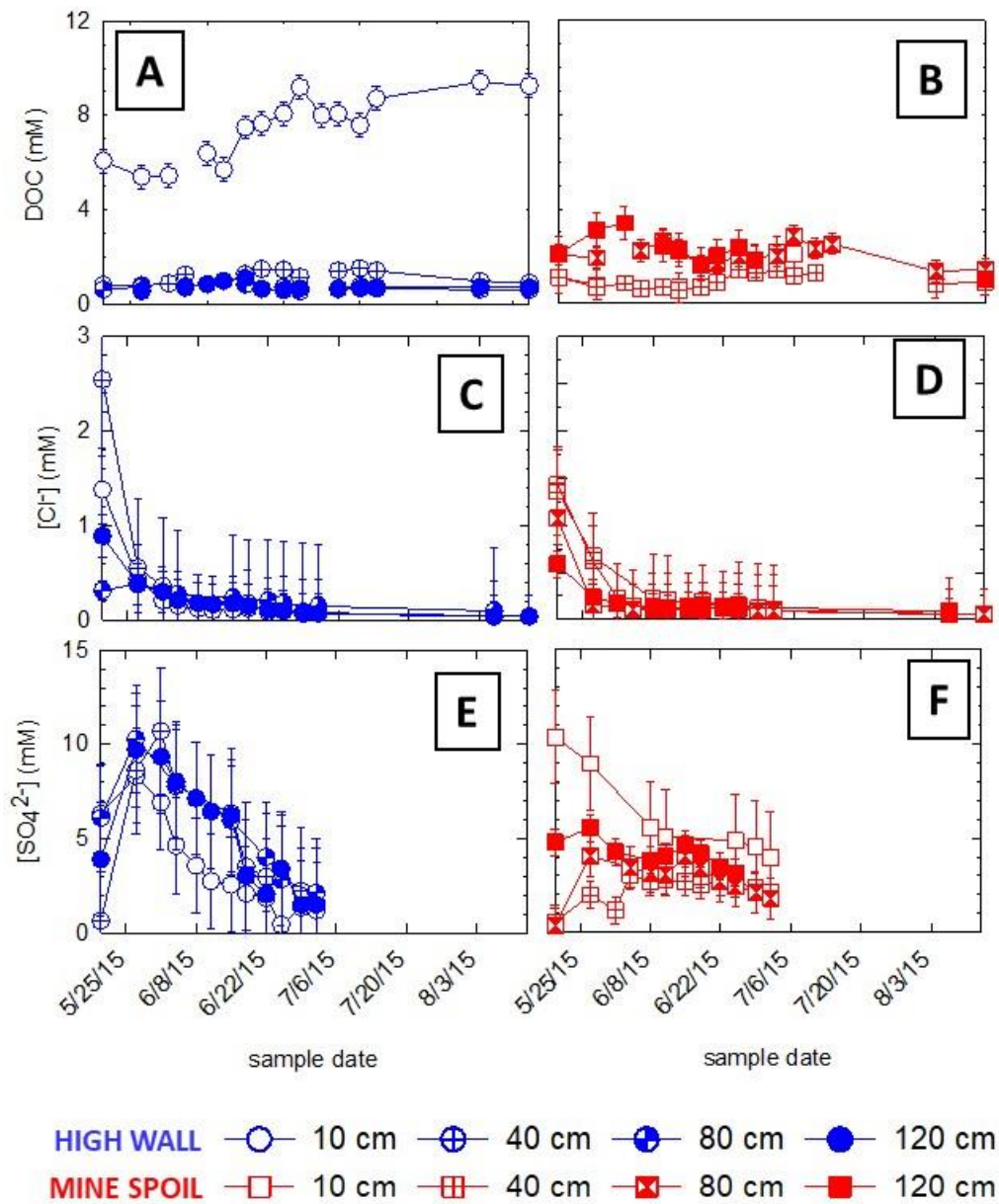


Figure S6. Aqueous concentrations of dissolved organic carbon (DOC) (A), chloride (B), and sulfate (C) collected from lysimeters installed in High Wall soils (blue circles, left) and Mine Spoil soils (red squares, center) over the sampling season for lysimeters installed at 10 cm (open), 40 cm (cross), 80 cm (hour glass), and 120 cm (filled).

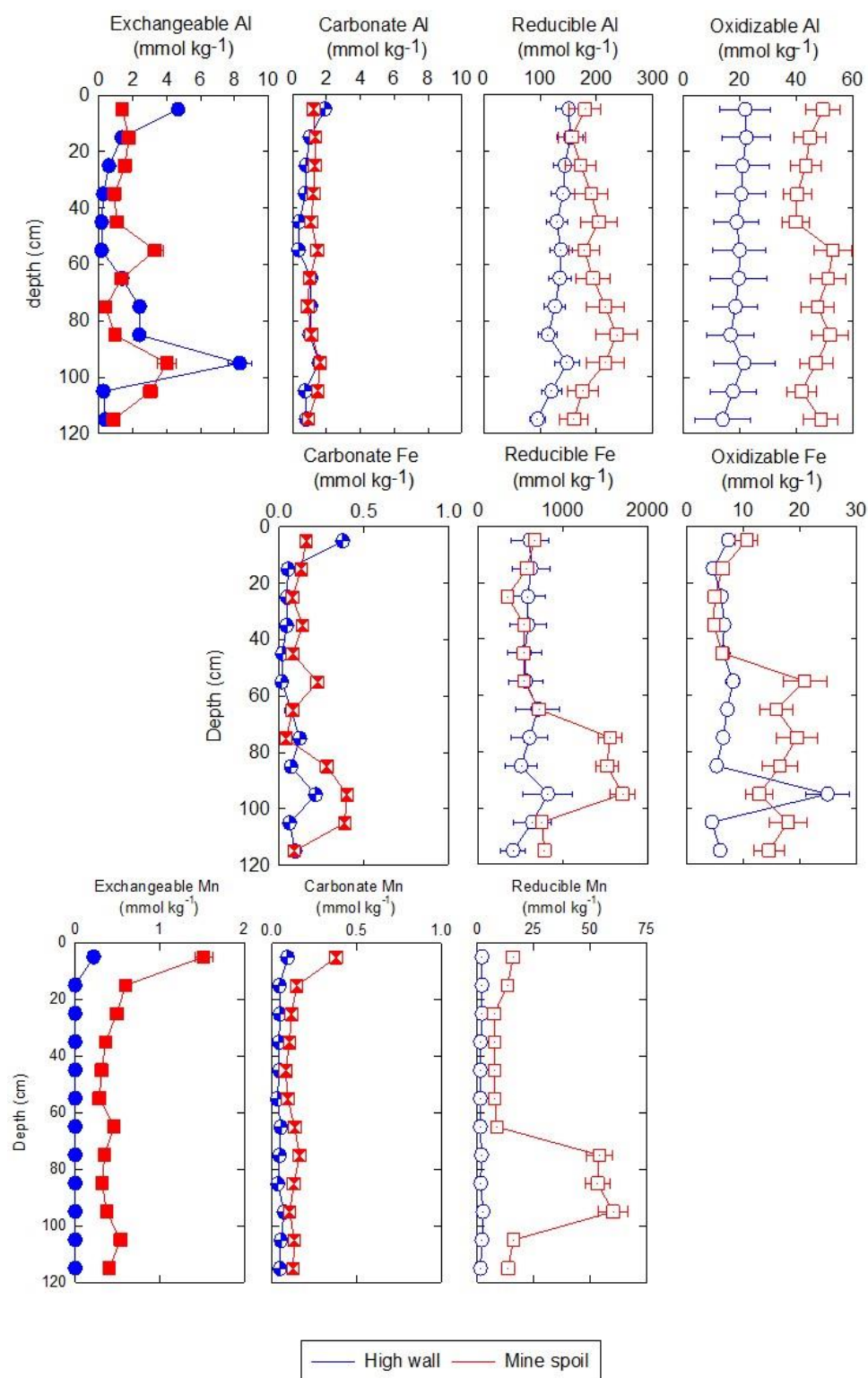


Figure S7. Sequential extraction scatter plot for Al (top), Fe (middle), and Mn (bottom) for the High Wall (red squares) and Mine Spoil (blue circles) for operationally defined exchangeable (closed), carbonate (hourglass), reducible (dotted), and oxidizable (open) components. Exchangeable Fe and reducible Mn were below detection limits for both soil cores.

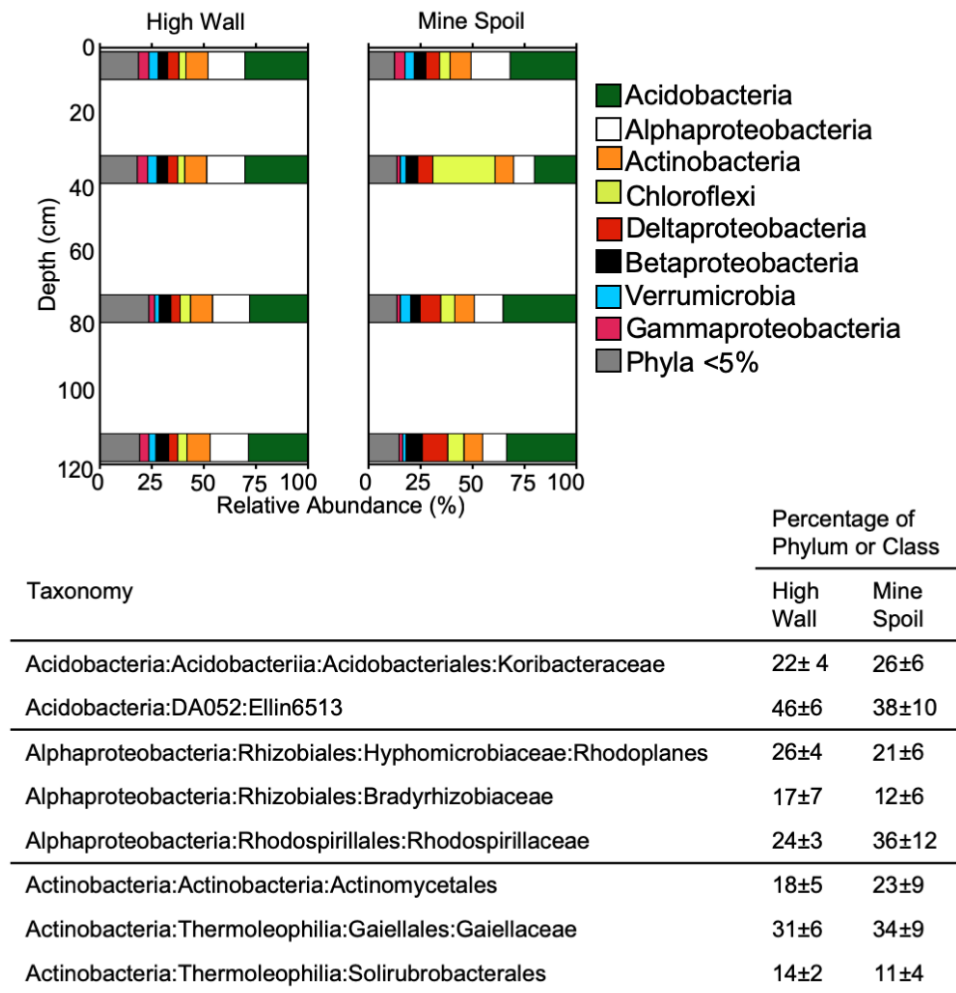


Figure S8. Relative abundances of phyla (and classes in the case of Proteobacteria) detected at different depths in High Wall and Mine Tailing samples. The table shows the mean relative abundances (within phylum or class) of most abundant taxa detected within the Acidobacteria, Alphaproteobacteria, and Actinobacteria.